

# Partial MCT1 invalidation protects against diet-induced non-alcoholic fatty liver disease and the associated brain dysfunction

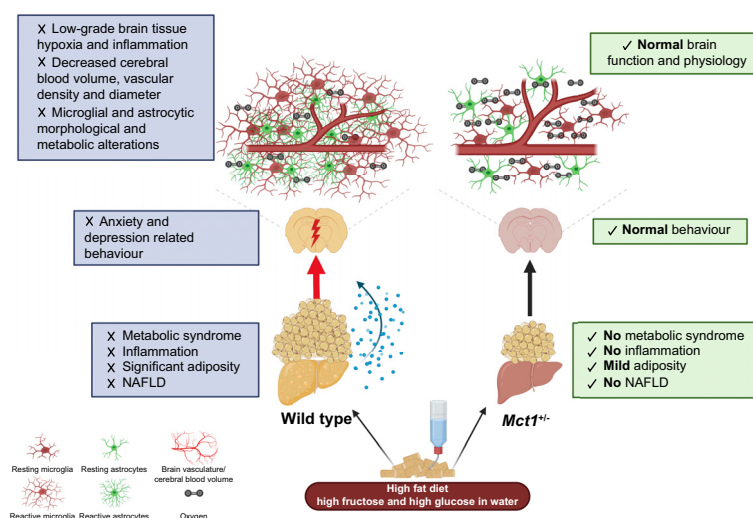
## Authors

Anna Hadjihambi, Christos Konstantinou, Jan Klohs, ..., Rajiv Jalan, Rosa Chiara Paolicelli, Luc Pellerin

## Correspondence

a.hadjichambi@researchinliver.org.uk (A. Hadjihambi), luc.pellerin@univ-poitiers.fr (L. Pellerin).

## Graphical abstract



## Highlights

- Diet-induced NAFLD and associated systemic alterations result in behavioural changes and low-grade brain tissue hypoxia.
- Brain hypoxia is likely linked to the induced low-grade brain inflammation, as well as cerebrovascular, glial, and metabolic alterations.
- *Mct1* haploinsufficient mice are protected from NAFLD and detrimental cerebral alterations.
- MCT1 is a potential novel therapeutic target for preventing and/or treating NAFLD and the associated multifactorial encephalopathy.

## Impact and implications

This study is focused on unravelling the pathophysiological mechanism by which cerebral dysfunction and cognitive decline occurs during NAFLD and exploring the potential of monocarboxylate transporter-1 (MCT1) as a novel preventive or therapeutic target. Our findings point to NAFLD as a serious health risk and its adverse impact on the brain as a potential global health system and economic burden. These results highlight the utility of *Mct1* transgenic mice as a model for NAFLD and associated brain dysfunction and call for systematic screening by physicians for early signs of psychological symptoms, and an awareness by individuals at risk of these potential neurological effects. This study is expected to bring attention to the need for early diagnosis and treatment of NAFLD, while having a direct impact on policies worldwide regarding the health risk associated with NAFLD, and its prevention and treatment.

# Partial MCT1 invalidation protects against diet-induced non-alcoholic fatty liver disease and the associated brain dysfunction

Anna Hadjihambi<sup>1,2,3,\*</sup>, Christos Konstantinou<sup>2,3</sup>, Jan Klohs<sup>4,5</sup>, Katia Monsorno<sup>1</sup>, Adrien Le Guennec<sup>6</sup>, Chris Donnelly<sup>1,7</sup>, I. Jane Cox<sup>2,3</sup>, Anjali Kusumbe<sup>8</sup>, Patrick S. Hosford<sup>9</sup>, Ugo Soffientini<sup>2,3</sup>, Salvatore Lecca<sup>10</sup>, Manuel Mameli<sup>10,11</sup>, Rajiv Jalan<sup>12</sup>, Rosa Chiara Paolicelli<sup>1</sup>, Luc Pellerin<sup>1,13,\*</sup>

Journal of Hepatology 2022. vol. ■ | 1–11

**Background & Aims:** Non-alcoholic fatty liver disease (NAFLD) has been associated with mild cerebral dysfunction and cognitive decline, although the exact pathophysiological mechanism remains ambiguous. Using a diet-induced model of NAFLD and monocarboxylate transporter-1 (*Mct1*<sup>+/-</sup>) haploinsufficient mice, which resist high-fat diet-induced hepatic steatosis, we investigated the hypothesis that NAFLD leads to an encephalopathy by altering cognition, behaviour, and cerebral physiology. We also proposed that global MCT1 downregulation offers cerebral protection.

**Methods:** Behavioural tests were performed in mice following 16 weeks of control diet (normal chow) or high-fat diet with high fructose/glucose in water. Tissue oxygenation, cerebrovascular reactivity, and cerebral blood volume were monitored under anaesthesia by multispectral optoacoustic tomography and optical fluorescence. Cortical mitochondrial oxygen consumption and respiratory capacities were measured using *ex vivo* high-resolution respirometry. Microglial and astrocytic changes were evaluated by immunofluorescence and 3D reconstructions. Body composition was assessed using EchoMRI, and liver steatosis was confirmed by histology.

**Results:** NAFLD concomitant with obesity is associated with anxiety- and depression-related behaviour. Low-grade brain tissue hypoxia was observed, likely attributed to the low-grade brain inflammation and decreased cerebral blood volume. It is also accompanied by microglial and astrocytic morphological and metabolic alterations (higher oxygen consumption), suggesting the early stages of an obesogenic diet-induced encephalopathy. *Mct1* haploinsufficient mice, despite fat accumulation in adipose tissue, were protected from NAFLD and associated cerebral alterations.

**Conclusions:** This study provides evidence of compromised brain health in obesity and NAFLD, emphasising the importance of the liver–brain axis. The observation of the protective effect of *Mct1* haploinsufficiency points to this protein as a novel therapeutic target for preventing and/or treating NAFLD and the associated brain dysfunction.

© 2022 The Author(s). Published by Elsevier B.V. on behalf of European Association for the Study of the Liver. This is an open access article under the CC BY license (<http://creativecommons.org/licenses/by/4.0/>).

## Introduction

Non-alcoholic fatty liver disease (NAFLD) is a metabolic syndrome, affecting approximately 25% of the population and >80% of morbidly obese people. Over the last decade, NAFLD has become known as a multisystem disease, affecting extra-hepatic organs, with its clinical burden not only confined to liver-related morbidity and mortality.<sup>1</sup> Indeed, the most common liver-related complication of individuals with NAFLD with advanced liver disease (F3/F4) that has progressed to decompensation over a long follow-up period, is hepatic encephalopathy.<sup>2</sup>

Several studies have reported the negative effects of unhealthy diet and obesity on cerebral function and cognition.<sup>3</sup> It is now clear that not only advanced forms of chronic liver disease, but even precirrhotic stages of NAFLD can be linked to

impaired cognitive performance<sup>4</sup> and cerebral function<sup>5</sup> (independently of cardiometabolic disorders), altered behaviour,<sup>6</sup> and low total cerebral volume.<sup>4</sup> These combine to compromise brain health.<sup>7,8</sup> However, more precise alterations of cerebral physiology and the mechanisms behind them are yet to be determined.

To function, the brain depends on continuous delivery of oxygen and energy substrates. The cerebral vasculature is well suited for this purpose, and additional mechanisms have evolved to closely regulate blood flow, matching oxygen supply with demand.<sup>9</sup> Therefore, any changes in these mechanisms or the structure of the cerebrovascular system can have detrimental effects on brain tissue oxygenation and overall physiology.<sup>10</sup> Several studies have reinforced this view by

Keywords: Non-alcoholic fatty liver disease; Hepatic encephalopathy; Cerebral oxygenation; Brain inflammation; Microglia; Astrocytes; Anxiety; Depression; Monocarboxylate transporter 1; Metabolism; Cerebral protection.

Received 17 November 2021; received in revised form 30 July 2022; accepted 5 August 2022; available online xxx

\* Corresponding authors. Addresses: The Roger Williams Institute of Hepatology London, Foundation for Liver Research, London, UK. Tel.: +44 207 255 9852. (A. Hadjihambi), or Inserm U1313, Université de Poitiers et CHU de Poitiers, France. Tel.: +33 5 49 44 47 79. (L. Pellerin).

E-mail addresses: [a.hadjichambi@researchinliver.org.uk](mailto:a.hadjichambi@researchinliver.org.uk) (A. Hadjihambi), [luc.pellerin@univ-poitiers.fr](mailto:luc.pellerin@univ-poitiers.fr) (L. Pellerin).

<https://doi.org/10.1016/j.jhep.2022.08.008>



ELSEVIER

## Mct1 haploinsufficiency protects against NAFLD

highlighting an association of cerebral hypoxia with neurodegenerative conditions, either predisposing the brain for developing neurodegeneration or occurring as the disease progresses.<sup>11</sup>

Recently, it has been observed that hypoxia not only directly induces neuronal damage, but also initiates cerebral inflammation through microglial and astrocytic responses.<sup>12</sup> Toxic inflammatory mediators produced by glial cells under hypoxic conditions are key in the development of brain inflammation, which exacerbates neuronal injury, synaptic remodelling, and neurodegeneration.<sup>13</sup> Growing evidence implicates low-grade chronic systemic inflammation and consequently brain inflammation in the pathogenesis of diet-induced obesity and cerebral dysfunction.<sup>14</sup> However, brain tissue oxygenation and the role of NAFLD in any detected alterations have yet to be investigated directly.

The monocarboxylate transporter-1 (MCT1, or SLC16A1) is a carrier of short-chain fatty acids, ketone bodies, and lactate in several tissues, playing an important role in energy homeostasis.<sup>15</sup> As previously shown, genetically modified mice haploinsufficient for *Mct1*<sup>+/-</sup> developed normally but exhibited a unique phenotype on a high-fat diet (HFD), characterised by resistance to hepatic steatosis and associated metabolic alterations, with some of the possible protective mechanisms described.<sup>16,17</sup>

In this study, we tested the hypothesis that NAFLD and associated systemic abnormalities lead to the development of an encephalopathy by altering cerebral physiology and behaviour. We also investigated whether a global MCT1 down-regulation, which prevents NAFLD development, may offer cerebral protection. Using an animal model of diet-induced NAFLD, and the *Mct1* haploinsufficient mouse line described above, we obtained data from a battery of *in vivo* and *ex vivo* studies, which suggest that NAFLD in the presence of obesity is associated with low-grade brain tissue hypoxia and inflammation, as well as cerebrovascular, metabolic, and behavioural changes, indicating early stages of an obesogenic diet-induced encephalopathy. *Mct1* haploinsufficient mice, despite fat accumulation in adipose tissue, were protected, indicating the potential for MCT1 as a novel preventive or therapeutic target.

## Materials and methods

All experiments were performed in accordance with the Swiss animal welfare laws approved by the Committee on Animal Experimentation for the Canton of Vaud, Switzerland (VD 3401.c) and the ARRIVE guidelines.<sup>18</sup> Further technical details on all experimental tests used are available in the [Supplementary material](#).

### Animal model

*Mct1*<sup>+/-</sup> mice<sup>17</sup> were bred in the animal facility of the Biomedical Sciences department at the University of Lausanne, Switzerland, to produce male *Mct1*<sup>+/-</sup> and *Mct1*<sup>+/+</sup> littermate controls. Animals were group-housed in individually ventilated cages, enriched with rails and cardboard tubes, in a room of 20–22 °C, relative moisture 50–60%, and 12-h light–dark cycle (light 7 a.m. to 7 p.m.). At 8 weeks old, mice were given *ad libitum* access to either a standard diet of normal chow (NC;

3242.PX.F12, Granovit, Kaiseraugst, Switzerland) and water or a HFD (Cat no. TD.93075.PWD; adjusted calories diet [55% fat], Envigo, Harlan Teklad, Indianapolis, Indiana, USA) with fructose and glucose in their water (HFDHF/HG; 23.1 g/L D-fructose [10021753, Axonlab, Baden, Switzerland] + 18.9 g/L D-glucose [A3666,1000, PanReac AppliChem, Darmstadt, Germany]) for 16 weeks.

At the end of the 16 weeks, blood (plasma) via cardiac puncture, brain, and liver tissues were collected under terminal anaesthesia for further analysis.

### Body weight and composition measurements

Body composition was measured in all mice using EchoMRI (LLC, Houston, TX, USA), at week 0 and 16 of their feeding regime. At the end of the feeding duration, % fat mass and lean mass were compared between groups. Body weight was obtained weekly using a digital balance, and total food intake per mouse per cage was calculated at the end of the feeding period for animals on the HFDHF/HG diet.

### Behavioural experiments

#### Open field

Open field (OF) to assess anxiety-like behaviour was performed using an arena divided into virtual quadrants. Each mouse was placed in the centre and allowed to explore for 15 min. Average speed and total distance travelled were measured to assess locomotion, whereas anxiety was evaluated according to the time spent exploring the centre zone.

#### Forced Swim Test

Following OF and 1 resting day, depressive-like behaviour was assessed using the forced swim test (FST). Mice were individually placed in a glass cylinder and allowed to swim for 4 min. Duration of immobility (floating) was recorded.

### Brain tissue oxygen measurements

#### Optical fluorescence

Under isoflurane anaesthesia, tissue partial pressure of oxygen ( $PO_2$ ) was monitored in the somatosensory (forelimb) region of the cortex (S1FL ~0.5 mm below the cortical surface) by optical fluorescence technology (Oxylite™, Oxford Optronics, Oxford, UK). Following a 15-min recovery period, parenchymal  $PO_2$  sampling was started until a stable reading was achieved.

#### Blood gas manipulations

After baseline  $PO_2$  was recorded, systemic hypercapnia was induced by 10%  $CO_2$  inhalation (in 21%  $O_2$  with the gas balance made of nitrogen) for 5 min.

#### Multispectral optoacoustic tomography

In a different cohort of mice, brain tissue oxygenation was measured under isoflurane anaesthesia with the inVision 128 small animal multispectral optoacoustic tomography (MSOT) system (iThera Medical GmbH, Munich, Germany).

MSOT images (Fig. 1D) were reconstructed as described in the Supplementary material. Regions of interest (ROIs) were drawn over the left and right cortex on deoxygenated haemoglobin (Hb)/oxygenated haemoglobin ( $HbO_2$ ) maps using

ImageJ (NIH, USA). ROIs for each region were averaged. Tissue oxygenation as a measure of tissue oxygen saturation ( $SO_2$ ) of the ROIs was calculated by the following:

$$SO_{2(MSOT)} = HbO_2 / (Hb + HbO_2) \times 100$$

Cerebral blood volume (CBV) was calculated by the following:

$$CBV = Hb + HbO_2$$

### High-resolution respirometry

Brain homogenates (somatosensory cortex) were prepared in prechilled MiRO5 buffer and transferred into calibrated Oxygraph-2k (O2k, Oroboros Instruments, Innsbruck, Austria) 2-ml chambers, where oxygen concentration ( $\mu M$ ) and oxygen flux per tissue mass ( $pmol O_2 s^{-1} mg^{-1}$ ) were recorded. The established substrate, uncoupler, inhibitor titration (SUIT) protocol SUIT-008 (<https://www.mitofit.org/index.php/SUIT-008>) was used (Fig. S1).

Respiratory capacities were expressed as oxygen consumption per wet mass of tissue ( $pmol s^{-1} mg^{-1}$ ) or per protein mass ( $pmol s^{-1} \mu g^{-1}$ ) and corrected for residual oxygen consumption (ROX).

### Immunofluorescence staining

Mice were terminally anaesthetised with sodium pentobarbital (150 mg/kg i.p.) and transcardially perfused with ice-cold 0.9% sodium chloride solution followed by 4% paraformaldehyde (PFA) at 4 °C. Brain and liver were removed, post-fixed in PFA overnight, and kept in PBS until processed. Liver slices were stained for H&E (Supplementary material). Surface of lipid droplets was measured, and fat proportionate area (FPA; % of total tissue surface) was calculated. Immunofluorescence labelling of microglia and astrocytes was performed on 60  $\mu m$  brain slices. Sections were incubated overnight at 4 °C with primary antibodies (ionised calcium binding adaptor molecule 1 [Iba1], 1:1,000, 019-19741, FUJIFILM Wako, Neuss, Germany; glial fibrillary acidic protein [GFAP], 1:500, Z0334, Dako, Santa Carla, California) and incubated with secondary antibodies (2 h at room temperature; Alexa Fluor Plus 555, Donkey anti-Rabbit, 1:1000, A32794, Thermo Fisher, Basel, Switzerland). Nuclei were labelled by incubation with Hoechst 33342 (1:10,000; ab228551; Abcam, Cambridge, UK) for 10 min at room temperature. Sections were imaged using a Zeiss LSM 700 confocal microscope (Jena, Germany) at 20 $\times$  and 60 $\times$  magnification. Semi-automated analysis was performed using ImageJ on 20 $\times$  magnification images evaluating cell density and % area fraction of Iba1/GFAP positive cells. Confocal stacks acquired with 60 $\times$  magnification were reconstructed in 3D using Imaris software (Bitplane, Schlieren, Switzerland) based on Iba1 intensity, and volume of individual cells was assessed.

### Statistical analysis

Oxygen measurements via optical fluorescence were digitised using a Power 1401 interface (CED, Cambridge, UK) and

processed using Spike 2 software (CED, Cambridge, UK). Statistical analysis was performed using GraphPad Prism (GraphPad Software, San Diego, California, USA). Data are expressed as mean  $\pm$  SEM. Differences were ascertained by 1-way or 2-way ANOVA followed by Tukey's multiple-comparisons *post hoc* test, the Mann-Whitney *U* test, or the Kruskal-Wallis test followed by Dunn's multiple-comparisons *post hoc* test where appropriate. Differences with a *p* value of <0.05 were considered significant.

Sample sizes were calculated by Gpower 3 v3.1.9.2 (Heinrich-Heine-Universität Düsseldorf, Düsseldorf, Germany) using a 'means: ANOVA (2 groups)' test, with a desired power of 90% and a significance level of 5%. The effect size was calculated from brain oxygen measurements performed in a preliminary study (*n* = 3). Based on this calculation, *n* = 6–10 was used. The same calculations were performed for other experiments, when possible, to determine appropriate *n* numbers.

## Results

### Animal model characterisation

Following 16 weeks of HFDHF/HG administration, a significant increase in % fat mass was observed in *Mct1<sup>+/+</sup>* (*n* = 25, 36  $\pm$  1%, *p* < 0.0001) and *Mct1<sup>+/-</sup>* (*n* = 24, 25  $\pm$  2%, *p* < 0.0001) animals, compared with that in their analogous NC controls (*Mct1<sup>+/+</sup>* NC, *n* = 19, 12  $\pm$  1%; *Mct1<sup>+/-</sup>* NC, *n* = 15, 11  $\pm$  1%), with no changes in lean mass and total food intake between the groups (Fig. 2A–C). However, % fat mass in *Mct1<sup>+/-</sup>* HFDHF/HG animals was lower compared with *Mct1<sup>+/+</sup>* HFDHF/HG animals (*p* < 0.0001).

Liver histology confirmed the presence of hepatic steatosis (Fig. 2D–E) only in *Mct1<sup>+/+</sup>* HFDHF/HG mice, which was accompanied by an increase in total brain lipids (Table S1), plasma cytokines (Fig. S2D–H), obesity-related endocrine abnormalities (increase in leptin and insulin and decrease in glucagon-like peptide-1 [GLP-1]) compared with *Mct1<sup>+/+</sup>* NC controls (Fig. S2A–C), recapitulating features observed in obese individuals.<sup>19</sup> As previously established, *Mct1<sup>+/-</sup>* HFDHF/HG mice were resistant to hepatic steatosis development,<sup>16,17</sup> systemic inflammation, and hormonal abnormalities (Fig. 2D and E and Fig. S2), despite substantial adiposity.

### *Mct1<sup>+/+</sup>* but not *Mct1<sup>+/-</sup>* animals on HFDHF/HG experience a NAFLD-associated anxiety- and depression-related behaviour

At the end of the feeding regime, OF and FST were performed. Average speed and distance of exploration in OF were not different between groups (Fig. 3A and B) indicating preserved locomotion irrespective of diet and body composition. However, obese *Mct1<sup>+/+</sup>* HFDHF/HG animals with NAFLD spent significantly less time exploring the centre zone (*n* = 10, 41  $\pm$  5 s, *p* = 0.005) compared with *Mct1<sup>+/+</sup>* NC controls (*n* = 10, 93  $\pm$  12 s; Fig. 3C and D). *Mct1<sup>+/-</sup>* HFDHF/HG mice without NAFLD did not reveal the same anxiety-like behaviour, as they spent significantly more time exploring the centre zone (*n* = 8, 90  $\pm$  15 s, *p* = 0.01) compared with *Mct1<sup>+/+</sup>* HFDHF/HG mice, which



## Mct1 haploinsufficiency protects against NAFLD

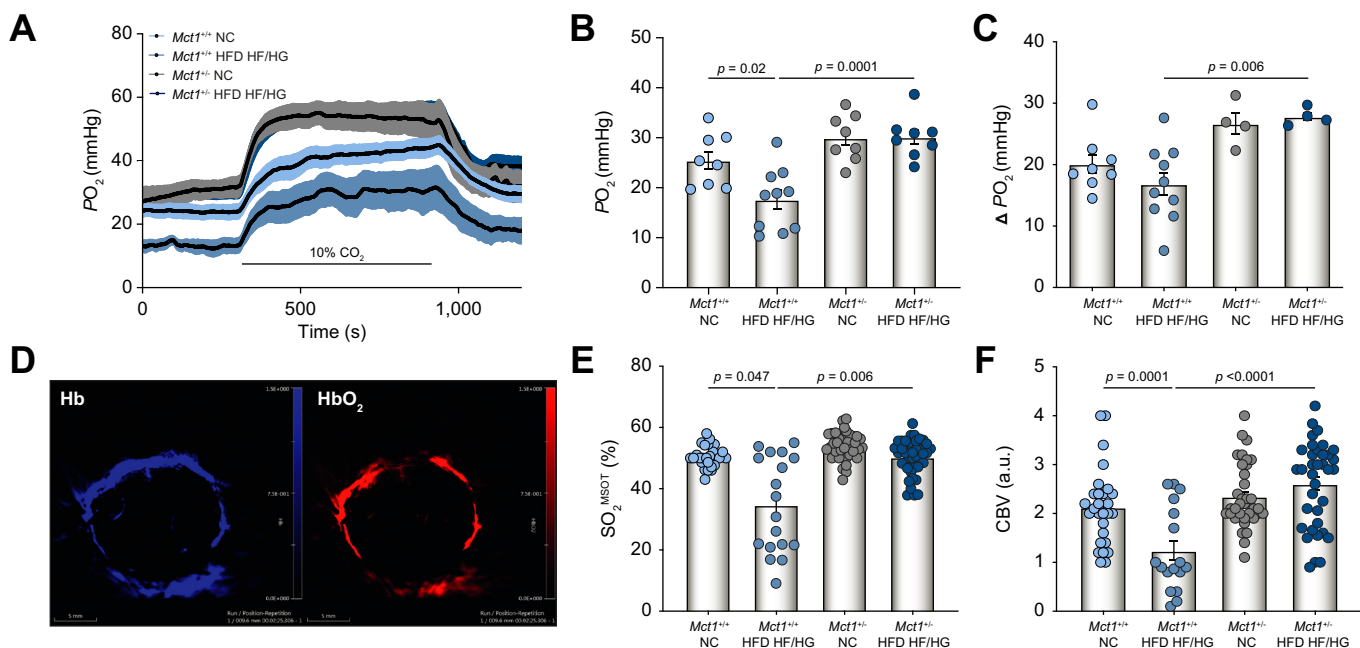


**Fig. 1. Cerebral oxygenation and cerebrovascular reactivity in *Mct1*<sup>+/+</sup> and *Mct1*<sup>+/-</sup> mice fed with NC or HFDHF/HG.** (A) Grouped data traces of  $PO_2$  measurements and quantification of (B) basal  $PO_2$  and (C) cerebrovascular reactivity to hypercapnia (10% inspired  $CO_2$ ) recorded via optical fluorescence in the somatosensory cortex of *Mct1*<sup>+/+</sup> and *Mct1*<sup>+/-</sup> mice fed with NC or HFDHF/HG. (D) Representative coronal maps of Hb and  $HbO_2$  *in vivo* with MSOT. Quantification of (E) brain tissue oxygen saturation and (F) CBV in the somatosensory cortex of *Mct1*<sup>+/+</sup> and *Mct1*<sup>+/-</sup> mice fed with NC or HFDHF/HG derived from Hb and  $HbO_2$  measurements. A  $p$  value of  $<0.05$  indicates significance level, 1-way ANOVA followed by Tukey's multiple-comparisons *post hoc* test and the Kruskal-Wallis test followed by Dunn's multiple-comparisons *post hoc* test. CBV, cerebral blood volume; Hb, deoxygenated haemoglobin;  $HbO_2$ , oxygenated haemoglobin; HFD, high-fat diet; HFDHF/HG, HFD with high fructose/glucose in water; MCT1, monocarboxylate transporter-1; MSOT, multispectral optoacoustic tomography; NC, normal chow;  $PO_2$ , partial pressure of oxygen.

was not different from *MCT*<sup>+/-</sup> NC controls ( $n = 7$ ,  $72 \pm 11$  s,  $p = 0.7$ ; Fig. 3C and D).

In the FST, obese *Mct1*<sup>+/+</sup> HFDHF/HG animals with NAFLD exhibited a significantly longer floating duration ( $n = 10$ ,  $84 \pm 7$  s,  $p = 0.01$ ) compared with *Mct1*<sup>+/+</sup> diet controls ( $n = 12$ ,  $51 \pm 6$  s; Fig. 3E), indicating a depression-related behaviour. *Mct1*<sup>+/-</sup> HFDHF/HG animals without NAFLD showed protection against depression development despite high fat mass, as seen by lower floating duration ( $n = 7$ ,  $6 \pm 3$  s,  $p < 0.0001$ ), compared with *Mct1*<sup>+/+</sup> HFDHF/HG mice, which was not significantly different from *Mct1*<sup>+/-</sup> NC controls ( $n = 11$ ,  $37 \pm 9$  s,  $p = 0.05$ ; Fig. 3E). These results are not attributable to changes in swimming abilities, which were not different between groups (Fig. 4C). No learning and memory deficits were detected in these mice (Fig. S3), in agreement with other animal studies.<sup>20</sup>

### *Mct1*<sup>+/+</sup> mice with NAFLD exhibit inflammation-associated changes in microglia and astrocytes, whereas *Mct1*<sup>+/-</sup> animals show protection

Obese *Mct1*<sup>+/+</sup> HFDHF/HG mice with NAFLD exhibited cortical microglial alterations, characterised by increased Iba1-positive cell density ( $n = 6$ ,  $86 \pm 4$  cells/ $1.8 \times 10^6 \mu m^3$ ,  $p = 0.003$ ), area covered (area fraction;  $n = 6$ ,  $37 \pm 3\%$ ,  $p = 0.0008$ ), and cell volume ( $n = 50$  cells,  $2 \pm 0.2 \mu m^3$ ,  $p < 0.0001$ ), compared with *Mct1*<sup>+/+</sup> NC controls (Fig. 4;  $n = 6$ ,  $58 \pm 6$  cells/ $1.8 \times 10^6 \mu m^3$ ;  $n = 6$ ,  $22 \pm 2\%$ ;  $n = 50$  cells,  $1 \pm 0.04 \mu m^3$ ). In contrast, *Mct1*<sup>+/-</sup> HFDHF/HG mice without NAFLD had normal microglial parameters (density:  $n = 6$ ,  $57 \pm 5$  cells/ $1.8 \times 10^6 \mu m^3$ ,  $p = 0.002$ ;

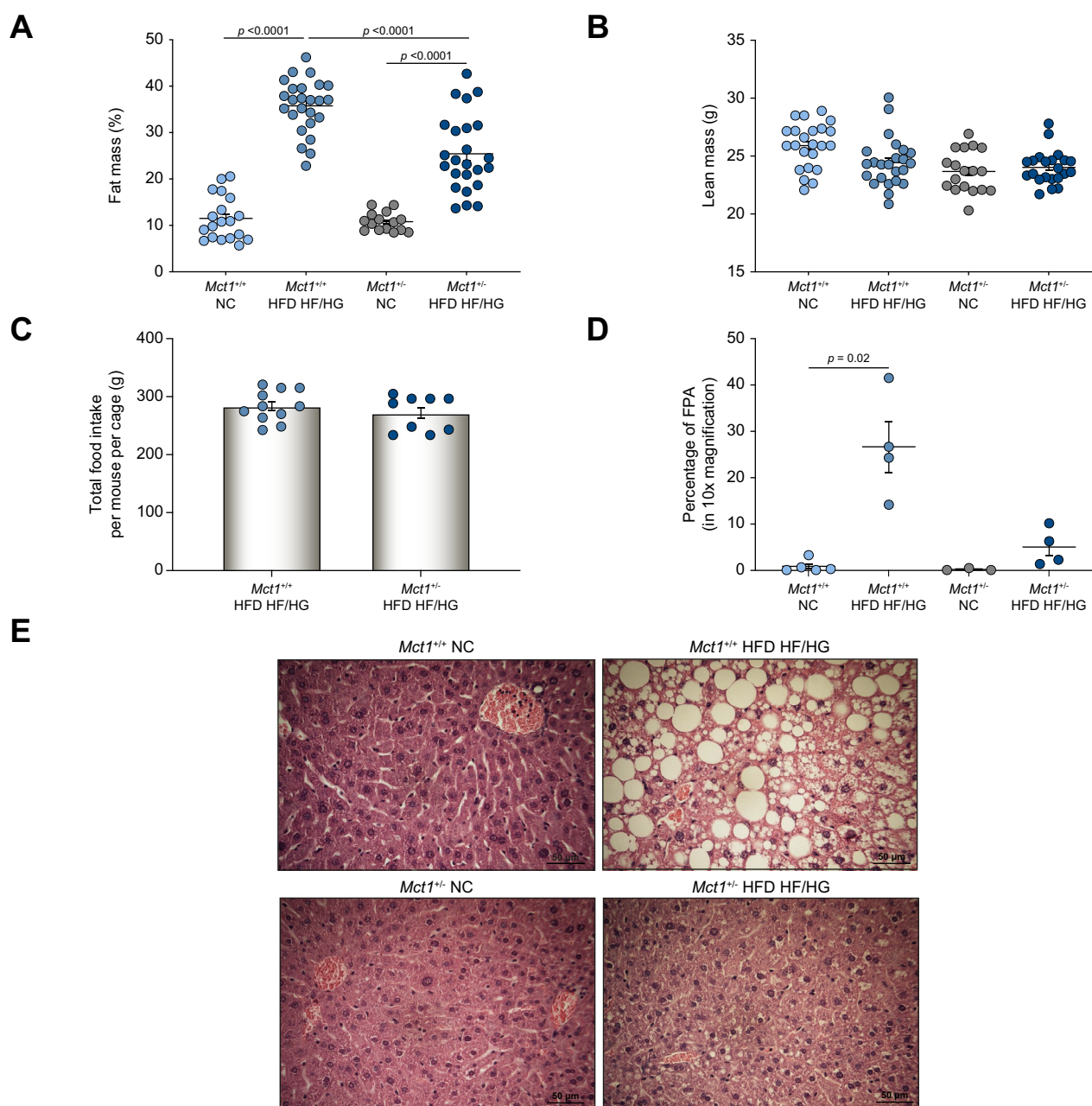
% area fraction:  $n = 6$ ,  $22 \pm 2\%$ ,  $p = 0.0005$ ; volume:  $n = 50$  cells,  $1 \pm 0.05 \mu m^3$ ,  $p < 0.0001$ ), which were similar to *Mct1*<sup>+/-</sup> NC controls (Fig. 4; density:  $n = 6$ ,  $54 \pm 4$  cells/ $1.8 \times 10^6 \mu m^3$ ,  $p = 0.9$ ; % area fraction:  $n = 6$ ,  $22 \pm 2\%$ ,  $p = 0.9$ ; volume:  $n = 50$  cells,  $1 \pm 0.05 \mu m^3$ ,  $p = 0.9$ ).

In the cortex of *Mct1*<sup>+/+</sup> HFDHF/HG mice, responsive astrocytes were detected by an increase in % area fraction of GFAP-positive cells ( $n = 6$ ,  $46 \pm 6\%$ ,  $p < 0.0001$ ) compared with *Mct1*<sup>+/+</sup> NC controls (Fig. 5;  $n = 6$ ,  $10 \pm 1\%$ ,  $p < 0.0001$ ). Like microglia, % area fraction of astrocytes was lower in *Mct1*<sup>+/-</sup> HFDHF/HG animals ( $n = 6$ ,  $8 \pm 3\%$ ,  $p < 0.0001$ ) compared with *Mct1*<sup>+/+</sup> HFDHF/HG mice and not different from *Mct1*<sup>+/-</sup> NC controls (Fig. 5;  $n = 6$ ,  $7 \pm 0.9\%$ ,  $p = 0.9$ ).

*Mct1*<sup>+/+</sup> HFDHF/HG mice also displayed an elevation in some cytokines (interferon gamma [IFN- $\gamma$ ] and IL-10 [Fig. S4]; no other cytokine alterations detected [Supplementary material]).

### Brain oxygenation is compromised in obese *Mct1*<sup>+/+</sup> mice with NAFLD, but not in *Mct1*<sup>+/-</sup> animals

Using an optic fibre oxygen sensor positioned above the somatosensory cortex, a lower  $PO_2$  was measured in obese *Mct1*<sup>+/+</sup> HFDHF/HG mice with NAFLD ( $n = 10$ ,  $18 \pm 2$  mmHg,  $p = 0.02$ ) compared with *Mct1*<sup>+/+</sup> NC controls ( $n = 8$ ,  $25 \pm 2$  mmHg; Fig. 1B). In contrast, *Mct1*<sup>+/-</sup> HFDHF/HG mice presented a similar  $PO_2$  ( $n = 8$ ,  $30 \pm 2$  mmHg,  $p = 0.9$ ) to *Mct1*<sup>+/-</sup> NC controls ( $n = 8$ ,  $30 \pm 2$  mmHg), which was significantly higher than in *Mct1*<sup>+/+</sup> HFDHF/HG animals ( $p = 0.0001$ , Fig. 1B). To evaluate the ability of cerebral vessels to respond to a

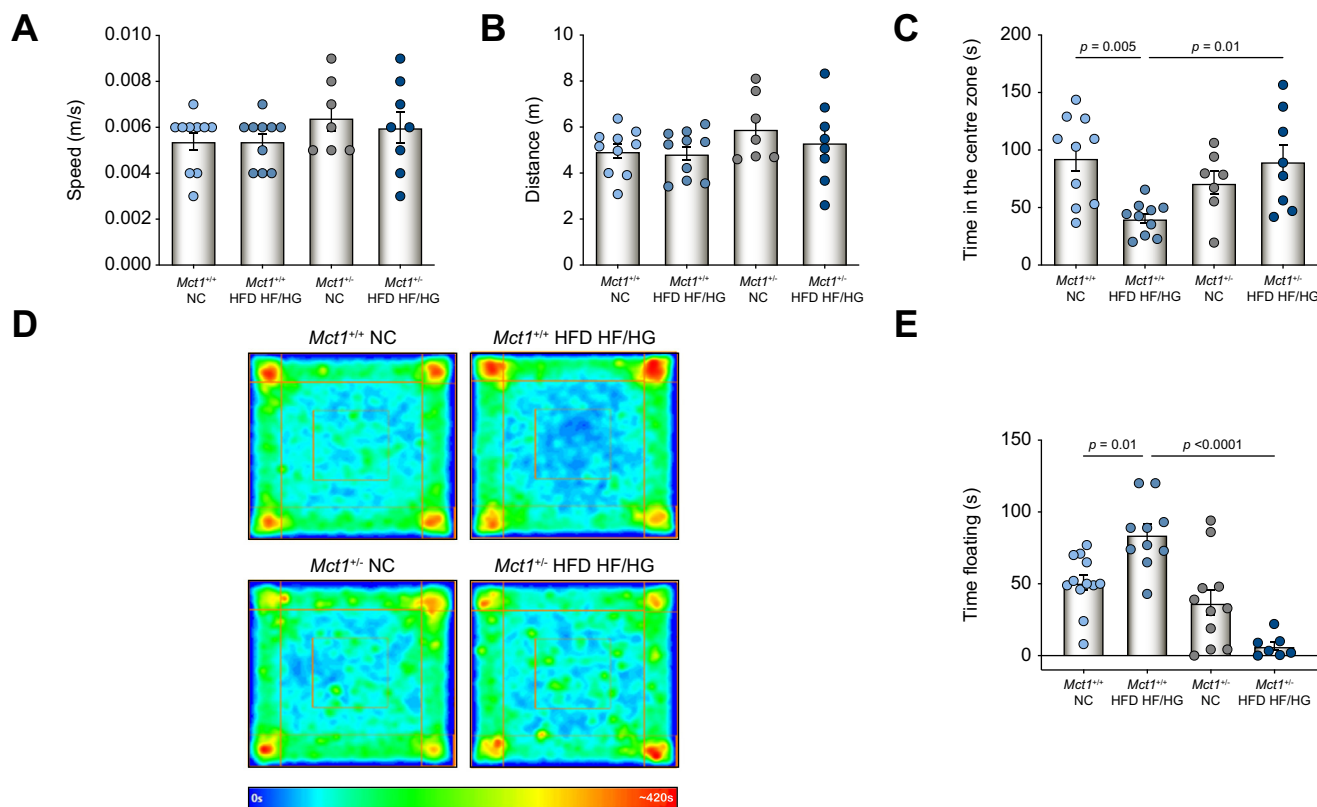


**Fig. 2. Characterisation of body composition and liver histology of mice fed with NC or HFDHF/HG.** (A) Percentage of fat mass and (B) lean mass assessed in  $Mct1^{+/+}$  and  $Mct1^{-/-}$  mice by EchoMRI at 16 weeks of either NC or HFDHF/HG diet. (C) Total HFD intake over a 16 weeks period per mouse per cage for  $Mct1^{+/+}$  and  $Mct1^{-/-}$  mice. (D) Quantitative histology analysis indicating percentage of FPA in liver slices of  $Mct1^{+/+}$  and  $Mct1^{-/-}$  mice fed with NC or HFDHF/HG diet. (E) Representative examples of FPA in liver slices of  $Mct1^{+/+}$  and  $Mct1^{-/-}$  mice fed with NC or HFDHF/HG diet. A  $p$  value of  $<0.05$  indicates significance level, the Mann-Whitney  $U$  test and 1-way ANOVA followed by Tukey's multiple-comparisons *post hoc* test and the Kruskal-Wallis test followed by Dunn's multiple-comparison *post hoc* test. FPA, fat proportionate area; HFD, high-fat diet; HFDHF/HG, HFD with high fructose/glucose in water; MCT1, monocarboxylate transporter-1; NC, normal chow.

known vasodilatory stimulus, hypercapnic acidosis was induced by changing the inspired gas mixture to include 10%  $\text{CO}_2$ , which led to a significant increase in parenchymal  $\text{PO}_2$  from baseline in all groups ( $p < 0.05$ ; Fig. 1A and C).

To exclude the impact of an acute inflammatory response following craniotomy, non-invasive MSOT was used to measure brain tissue oxygenation.  $Mct1^{+/+}$  HFDHF/HG mice with

NAFLD had a significantly lower  $\text{SO}_2$  ( $n = 3$ , 6 ROIs/animal,  $35 \pm 4\%$ ,  $p = 0.047$ ) compared with  $Mct1^{+/+}$  NC controls ( $n = 5$ , 6 ROIs/animal,  $51 \pm 1\%$ ; Fig. 1E).  $Mct1^{-/-}$  HFDHF/HG mice had normal levels of  $\text{SO}_2$  ( $n = 7$ , 6 ROIs/animal,  $50 \pm 1\%$ ,  $p = 0.06$ ) compared with  $Mct1^{-/-}$  NC controls ( $n = 6$ , 6 ROIs/animal,  $54 \pm 1\%$ ), which were higher than those of  $Mct1^{+/+}$  HFDHF/HG animals ( $p = 0.006$ ; Fig. 1E).

**Mct1 haploinsufficiency protects against NAFLD**

**Fig. 3. Assessment of anxiety- and depression-related behaviour in  $Mct1^{+/+}$  and  $Mct1^{+/-}$  mice fed with NC or HFDHF/HG.** Measurement of mean (A) speed, (B) distance, and (C) time spent by  $Mct1^{+/+}$  and  $Mct1^{+/-}$  mice fed with NC or HFDHF/HG exploring the centre zone of the arena, assessed by the OF test. (D) Representative heatmaps indicating the time spent by  $Mct1^{+/+}$  and  $Mct1^{+/-}$  mice fed with NC or HFDHF/HG exploring each zone during the OF test. (E) Measurement of time spent floating by  $Mct1^{+/+}$  and  $Mct1^{+/-}$  mice fed with NC or HFDHF/HG during the FST. A  $p$  value of  $<0.05$  indicates significance level, the Kruskal–Wallis test followed by Dunn’s multiple-comparisons *post hoc* test and 1-way ANOVA followed by Tukey’s multiple-comparisons *post hoc* test. FST, forced swim test; HFD, high-fat diet; HFDHF/HG, HFD with high fructose/glucose in water; MCT1, monocarboxylate transporter-1; NC, normal chow; OF, open field.

In  $Mct1^{+/+}$  HFDHF/HG mice, CBV (an indicator of blood/oxygen supply to the brain and vascular density) was significantly decreased ( $1 \pm 0.2$  a.u.,  $p = 0.04$ ) compared with  $Mct1^{+/+}$  NC controls ( $2 \pm 0.1$  a.u.; Fig. 1F), but cerebral blood flow (CBF), measured from arterial spin labelling magnetic resonance imaging (MRI), was unaltered (Fig. S5). The reduction in CBV was also associated with a reduction in vascular density (Fig. S6A and B) and a decrease in vessel diameter (Fig. S6C).  $Mct1^{+/-}$  HFDHF/HG mice had normal CBV ( $3 \pm 0.1$  a.u.), similar to  $Mct1^{+/-}$  NC controls ( $2 \pm 0.1$  a.u.,  $p = 0.5$ ), which was higher than that of  $Mct1^{+/+}$  HFDHF/HG animals ( $p = 0.0001$ ; Fig. 1F). Vascular density and vessel diameter were not significantly different between  $Mct1^{+/-}$  HFDHF/HG and  $Mct1^{+/-}$  NC animals (Fig. S6A–C).

**Obese  $Mct1^{+/+}$  animals with NAFLD present higher mitochondrial respiratory capacities but not improved metabolic outcome, whereas  $Mct1^{+/-}$  animals remain unaffected**

To investigate further the lower brain oxygenation observed in obese  $Mct1^{+/+}$  animals with NAFLD, oxygen consumption by mitochondrial respiration was measured *ex vivo* in homogenised cortical tissue (constant mass) using high-resolution respirometry.

For tissue mass-specific fluxes (Fig. 6A), only  $Mct1^{+/+}$  HFDHF/HG mice showed a significantly higher NADH pathway oxidative phosphorylation (OXPHOS) (P) capacity ( $N_p$ ) but no differences in OXPHOS ( $NS_p$ ) respiratory capacities compared with NC controls. Upon stepwise titration of the uncoupler carbonyl cyanide *p*-trifluoro-methoxyphenyl hydrazone (FCCP), there was a significantly higher combined NADH and succinate-linked pathway (NS) electron transfer (E) capacity in  $Mct1^{+/+}$  HFDHF/HG mice compared with controls and  $Mct1^{+/-}$  HFDHF/HG mice, which were not different from  $Mct1^{+/-}$  NC controls.

Despite the increase in cortical respiratory capacities of  $Mct1^{+/+}$  HFDHF/HG mice, no positive changes were observed in cerebral metabolite ratios measured by *ex vivo* nuclear magnetic resonance (NMR) spectroscopy (Table S2) or in protein content of OXPHOS complex subunits and proteins involved in mitochondrial remodelling (Fig. S7). Differences in respiratory capacities were eliminated when measurements were normalised to  $\mu\text{g}$  of protein/mg of brain tissue used (Fig. 6B).

**Discussion**

Individuals with NAFLD have been reported to experience cognitive impairment,<sup>8</sup> with the aetiology and precise cerebral dysfunction yet to be thoroughly characterised. In our study,



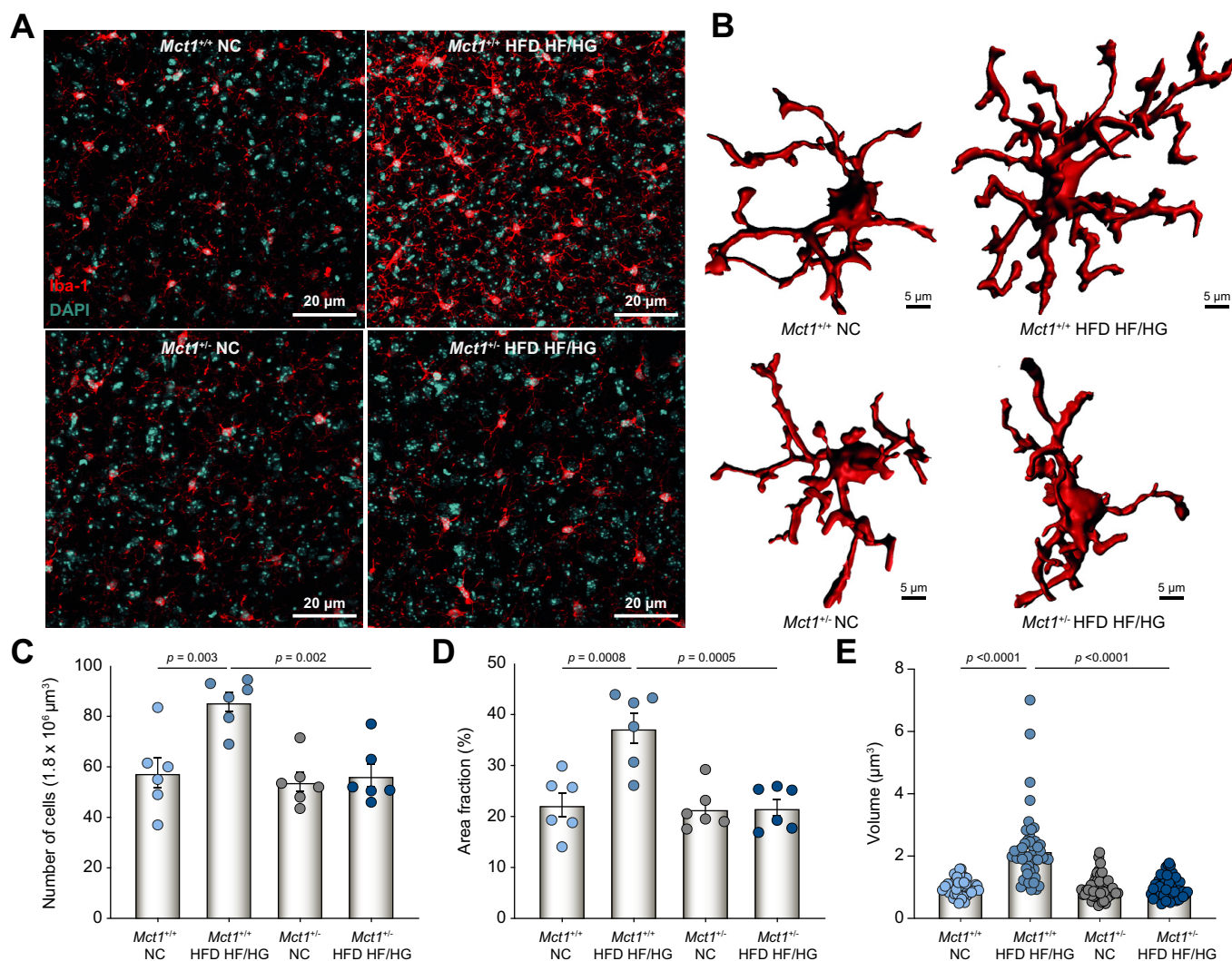


**Fig. 4. Determination of cortical microglial inflammatory response in  $Mct1^{+/+}$  and  $Mct1^{+/-}$  mice fed with NC or HFDHF/HG.** (A) Representative confocal z-stack projections and (B) 3D reconstruction of Iba1-positive microglial cells in the cortex of  $Mct1^{+/+}$  and  $Mct1^{+/-}$  mice fed with NC or HFDHF/HG. Quantification of (C) density, (D) percentage area fraction, and (E) volume of Iba1-positive microglia in the cortex of  $Mct1^{+/+}$  and  $Mct1^{+/-}$  mice fed with NC or HFDHF/HG. A p value of  $<0.05$  indicates significance level, 1-way ANOVA followed by Tukey's multiple-comparisons *post hoc* test and the Kruskal-Wallis test followed by Dunn's multiple-comparisons *post hoc* test. HFD, high-fat diet; HFDHF/HG, HFD with high fructose/glucose in water; Iba1, ionised calcium binding adaptor molecule 1; MCT1, monocarboxylate transporter-1; NC, normal chow.

HFDHF/HG caused obesity, hormonal and metabolic alterations, and NAFLD in  $Mct1^{+/+}$  animals, which resulted in specific brain clinico-pathological features. These features included anxiety- and depression-related behaviour, also reported in obese people<sup>21</sup> and those with NAFLD, which were even worse in the presence of insulin resistance<sup>22</sup> (as seen in  $Mct1^{+/+}$  HFDHF/HG mice). Additionally, low-grade brain tissue hypoxia, likely caused by the low-grade brain inflammation and decreased CBV, was accompanied by microglial and astrocytic morphological and metabolic alterations. Unlike  $Mct1^{+/+}$  mice, animals with a lower global expression of MCT1 ( $Mct1^{+/-}$ ) did not develop NAFLD or associated hormonal and metabolic alterations when fed with HFDHF/HG, despite the substantial fat accumulation in adipose tissue. Such phenotype allowed us to investigate the liver-brain interactions during HFDHF/HG and obesity, with data indicating that liver protection and associated induced systemic alterations, effectively prevent behavioural and cerebral dysfunction, emphasising the role of the

liver-brain axis in NAFLD-induced encephalopathy, that up until now was mainly attributed to obesity.

Adiposity is associated with increased secretion of inflammatory and fibrotic mediators, which can reach the liver and contribute to chronic low-grade inflammation,<sup>23</sup> while prompting brain inflammation, with astrocytes and microglia playing a pivotal role.<sup>24</sup> Indeed, obese  $Mct1^{+/+}$  animals with NAFLD presented peripheral and cerebral upregulation of certain pro- and anti-inflammatory cytokines, as well as remarkable alterations in cortical microglia (also seen in individuals with steatohepatitis<sup>25</sup>) and astrocytes, all of which were strikingly prevented in  $Mct1^{+/-}$  HFDHF/HG animals without NAFLD.

The morphological alterations of cortical microglia and astrocytes, as well as the moderate cytokine elevation, suggest that brain inflammation is mild with cells just undergoing a low-grade chronic response. IL-10, an anti-inflammatory cytokine, redirects active astrocytes to produce mediators, which



## Mct1 haploinsufficiency protects against NAFLD

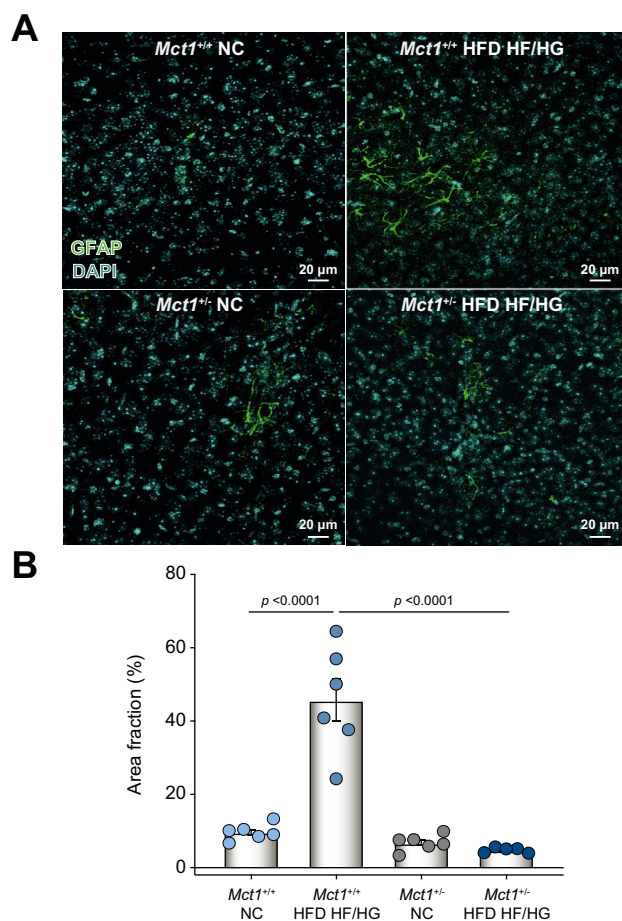


**Fig. 5. Determination of cortical astrocytic response in  $Mct1^{+/+}$  and  $Mct1^{+/-}$  mice fed with NC or HFDHF/HG.** (A) Representative confocal z-stack projections and (B) quantification of percentage area fraction of GFAP positive astrocytes in the cortex of  $Mct1^{+/+}$  and  $Mct1^{+/-}$  mice fed with NC or HFDHF/HG.  $p$  value of  $<0.05$  indicates significance level, one-way ANOVA followed by Tukey's multiple comparisons *post hoc* test.

attenuate microglial response.<sup>26</sup> IFN- $\gamma$  stimulates microglia and astrocytes to produce pro-inflammatory cytokines and chemokines.<sup>27</sup> However, the net effect of IFN- $\gamma$  signalling in the central nervous system (CNS) is similar to that in the periphery, also anti-inflammatory. Therefore, it is not clear whether the cellular response in  $Mct1^{+/+}$  HFDHF/HG mice is a pro- or anti-inflammatory reaction. Nonetheless, our results show that brain inflammation in diet-induced NAFLD extends to the cortex (beyond the hippocampus and hypothalamus as seen during obesity<sup>28</sup>), increasing the risk of cerebral damage as it persists. Brain inflammation can also occur when peripheral cytokines communicate with the brain across the intact blood-brain barrier (BBB), by activating the endothelium, which in turn signals to perivascular macrophages inducing further microglial response.

MCT1 is widely expressed in the brain,<sup>29</sup> and its role in promoting microglial response and associated pro-inflammatory effects by enhancing glycolysis has been shown.<sup>30</sup> In other conditions, such as ischaemia,<sup>31</sup> MCT1 expression is upregulated in responsive astrocytes. Therefore, it is possible that the partial invalidation of MCT1 (without compensation from other MCTs; Fig. S8) provides protection by preventing the above response processes. The involvement of the vagus nerve sensory afferents, direct active transport of cytokines across the BBB, compromised vascular permeability and alterations in the gut microbiome in developing brain inflammation,<sup>32</sup> and the possible protective role of MCT1 downregulation in these has not been investigated here but cannot be excluded as contributing factors.

Tissue inflammation and hypoxia share an interdependent relationship in the periphery and CNS during various pathologies.<sup>33</sup> NAFLD is characterised by a pro-inflammatory and pro-coagulant state that promotes processes that induce cerebrovascular damage and, consequently, contributes to clinical and subclinical cerebrovascular pathologies.<sup>34</sup> Using 2 lines of evidence (optical fluorescence and MSOT), we demonstrated that NAFLD is associated with reduced cortical

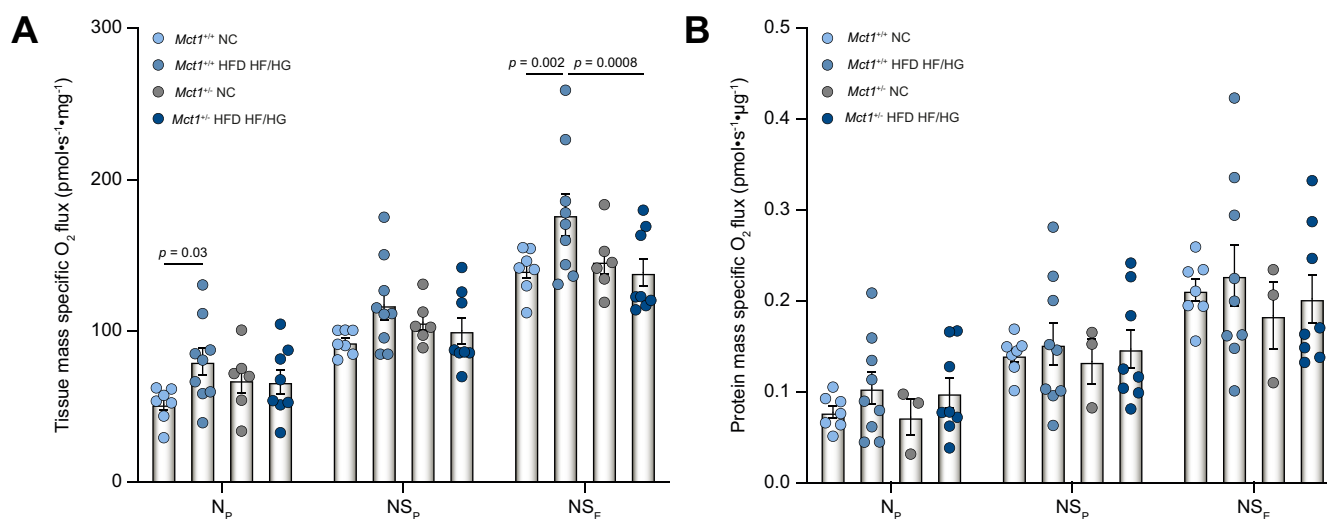


**Fig. 6. Determination of cortical mitochondrial respiratory capacities by high-resolution respirometry in  $Mct1^{+/+}$  and  $Mct1^{+/-}$  mice fed with NC or HFDHF/HG.** (A) Tissue mass and (B) protein mass specific oxygen fluxes in somatosensory cortical tissue samples from  $Mct1^{+/+}$  and  $Mct1^{+/-}$  mice fed with NC or HFDHF/HG: OXPHOS capacity ( $N_p$  and  $NS_p$ ) and E capacity ( $NS_E$ ). A  $p$  value of  $<0.05$  indicates significance level, 2-way ANOVA followed by Tukey's multiple-comparisons *post hoc* test. E, electron transfer; HFD, high-fat diet; HFDHF/HG, HFD with high fructose/glucose in water; MCT1, monocarboxylate transporter-1; NC, normal chow;  $N_p$ , NADH pathway OXPHOS capacity;  $NS$ , NADH and succinate-linked pathway; OXPHOS, oxidative phosphorylation; P, OXPHOS.

tissue oxygenation, which was only observed in *Mct1*<sup>+/-</sup> HFDHF/HG mice, that also displayed lower cortical CBV.

In these mice, CBF, which is the product of volume and velocity of blood flowing through the brain, was not significantly decreased. This could be as a result of the early stages of the disease and the compensatory action of high blood pressure (Fig. S9) observed in *Mct1*<sup>+/-</sup> HFDHF/HG mice. Elevated transmitted cerebral blood velocity (as blood volume was decreased and CBF was constant) results in potentially harmful pulsatile energy to be transferred to the microvasculature leading to damage, contributing to the decreased CBV. Additionally, the observed decrease in vascular density and vessel diameter in the cortex of *Mct1*<sup>+/-</sup> HFDHF/HG mice could further compromise blood/oxygen supply, contributing to the reported low-grade hypoxia. These vascular alterations may occur owing to volume changes associated with the reported glial responses, either as a compensatory mechanism to preserve the extracellular space volume and avoid oedema or as a consequence of compression. As these vascular alterations were also associated with an increase in average distance between 2 vessels in close proximity (Fig. S6D), the impact of increased oxygen diffusion distance and therefore limited oxygen diffusion range within the tissue, contributing to the observed brain hypoxia, cannot be excluded. Despite this decrease in vessel diameter, cerebrovascular reactivity was preserved, suggesting that remaining vessels are still functional, indicating a potential for restoring brain oxygenation by cerebrovascular dilation, as long as vascular density does not decline dramatically. The additional impact of an altered vascular tone cannot be excluded. The preserved cerebrovascular reactivity also indicates an overall preserved pericyte viability (lack of death in rigor) and function, as they normally respond to CO<sub>2</sub> by inducing capillary dilation, contributing to the increase in CBF and brain oxygenation.<sup>35</sup>

Although *Mct1*<sup>+/-</sup> HFDHF/HG animals also have reduced (but not significant) vascular density, they have a normal vessel diameter. In parallel, *in vivo* electrophysiology recordings (Fig. S10A) indicate a higher neuronal firing rate in these animals. These results together suggest a compensatory mechanism, via the neurovascular coupling, by which the increase in firing activity results in vasodilation during active brain states but returns to normal diameter when CNS depression is achieved by pentobarbital overdose<sup>36</sup> during fixation. Therefore, despite the small decrease in density, CBV and oxygenation are maintained at normal levels in *Mct1*<sup>+/-</sup> HFDHF/HG animals.

Our results also suggest that the observed alterations in glial cells contribute further to (and possibly become exacerbated by) the decrease in brain tissue oxygenation observed in obese *Mct1*<sup>+/-</sup> animals with NAFLD. Higher respiratory capacity (*i.e.* oxygen consumption) was recorded in the cortex of these mice, which was eliminated when the measurements were normalised to micrograms of protein per milligram of brain tissue used. As the protein content of OXPHOS complex subunits and proteins involved in mitochondrial remodelling were unchanged, it is likely that only functional changes are responsible for the higher respiratory capacities when normalised to tissue mass. Neurons are unlikely to contribute to the oxygen consumption changes as *in vivo* extracellular single-unit recordings indicated no differences in cortical neuronal activity between

obese *Mct1*<sup>+/-</sup> animals with NAFLD and *Mct1*<sup>+/-</sup> NC controls (Fig. S10A and B). However, as neuronal excitability can be slightly altered in *Mct1*<sup>+/-</sup> mice by the diet, it cannot be excluded that this aspect contributes to modifying brain responses to peripheral signals.

*Mct1*<sup>+/-</sup> HFDHF/HG mice without NAFLD showed protection against all cerebral alterations. These mice did not experience brain inflammation and glial alterations, explaining the normal respiratory capacities and oxygen consumption. As *Mct1*<sup>+/-</sup> HFDHF/HG mice develop fat accumulation but not NAFLD, metabolic syndrome, or systemic inflammation, it is suggested that the protection against cerebral alterations is partly caused by the absence of liver disease, emphasising its importance in studies focusing on obesity. Furthermore, because these mice presented less fat accumulation in the adipose tissue compared with *Mct1*<sup>+/-</sup> HFDHF/HG animals, and because of the absence of metabolic syndrome, it implies that no substantial damage has occurred yet to trigger the damaging inflammatory and cerebrovascular alterations seen in *Mct1*<sup>+/-</sup> mice, which exhibit higher % fat mass.

MCT1 is found in several other tissues including muscles, adipose tissue, heart, and intestine, all of which are involved in energy homeostasis regulations<sup>37</sup> and are altered during obesity and NAFLD. These organs can communicate with the brain, and therefore, their contributing role in the reported protective phenotype cannot be ruled out when using mice with global haploinsufficiency. Additionally, the partial invalidation of MCT1 has an impact on the immune system in the periphery (considering its role in immune cell function<sup>38</sup>), and it might participate in the beneficial effects observed by reducing peripheral inflammation and consequently preserving brain function. Similarly, other glial cells in the CNS, such as tanycytes, which have been shown to express MCT1<sup>39</sup> and be implicated in the control of systemic metabolism by acting as glucose<sup>40</sup> and lipid<sup>41</sup> sensors, are also likely to participate in the phenotype of resistance to diet-induced NAFLD. Conditional knockdown models in future studies will allow answers to these questions. Further limitations include the lack of precise mechanistic pathway responsible for the protective phenotype. The impact of other pathological factors, such as ammonia, and the reversibility of NAFLD and induced encephalopathy by partial blockage of MCT1 will need to be investigated further.

In conclusion, this study provides evidence indicating a key role of NAFLD in inducing low-grade brain tissue hypoxia and inflammation, as well as cerebrovascular, glial, metabolic, and behavioural alterations. Such effects are expected to persist chronically or even worsen with disease progression, leading to the early stages of a NAFLD-induced brain dysfunction, while increasing the risk of neurodegenerative conditions, such as Alzheimer's disease, that share the above pathophysiological mechanisms.<sup>42</sup> *Mct1* haploinsufficient mice, despite fat accumulation in adipose tissue, were protected from NAFLD and the above detrimental cerebral alterations, emphasising the importance of the liver-brain axis in developing cognitive decline observed in obese individuals. Finally, this protective phenotype indicates the potential of MCT1 as a novel therapeutic target for preventing and/or treating NAFLD and the associated multifactorial encephalopathy.

## Mct1 haploinsufficiency protects against NAFLD

## Affiliations

<sup>1</sup>Department of Biomedical Sciences, University of Lausanne, Lausanne, Switzerland; <sup>2</sup>The Roger Williams Institute of Hepatology London, Foundation for Liver Research, London, UK; <sup>3</sup>Faculty of Life Sciences and Medicine, King's College London, London, UK; <sup>4</sup>Institute for Biomedical Engineering, University of Zurich and ETH Zurich, Zurich, Switzerland; <sup>5</sup>Neuroscience Centre Zurich, University of Zurich and ETH Zurich, Zurich, Switzerland; <sup>6</sup>NMR Facility, Guy's Campus, King's College London, London, UK; <sup>7</sup>Institute of Sports Science, University of Lausanne, Lausanne, Switzerland; <sup>8</sup>Tissue and Tumor Microenvironments Group, MRC Human Immunology Unit, MRC Weatherall Institute of Molecular Medicine, University of Oxford, Oxford, UK; <sup>9</sup>Centre for Cardiovascular and Metabolic Neuroscience, Neuroscience, Physiology and Pharmacology, University College London, London, UK; <sup>10</sup>The Department of Fundamental Neuroscience, University of Lausanne, Lausanne, Switzerland; <sup>11</sup>Inserm, UMR-S 839, Paris, France; <sup>12</sup>Institute for Liver and Digestive Health, Division of Medicine, UCL Medical School, Royal Free Hospital, University College London, London, UK; <sup>13</sup>Inserm U1313, Université de Poitiers et CHU de Poitiers, France

## Abbreviations

BBB, blood–brain barrier; CBF, cerebral blood flow; CBV, cerebral blood volume; CNS, central nervous system; E, electron transfer; FCCP, carbonyl cyanide *p*-tri-fluoro-methoxyphenyl hydrazone; FPA, fat proportionate area; FST, forced swim test; GFAP, glial fibrillary acidic protein; GLP-1, glucagon-like peptide-1; Hb, deoxygenated haemoglobin; HbO<sub>2</sub>, oxygenated haemoglobin; HFD, high-fat diet; HFDHF/HG, HFD with high fructose/glucose in water; Iba1, ionised calcium binding adaptor molecule 1; IFN- $\gamma$ , interferon gamma; MCT1, monocarboxylate transporter-1; MRI, magnetic resonance imaging; MSOT, multispectral optoacoustic tomography; N, NADH-linked pathway; NAFLD, non-alcoholic fatty liver disease; NC, normal chow; NMR, nuclear magnetic resonance; N<sub>p</sub>, NADH pathway OXPPOS capacity; NS, NADH and succinate-linked pathway; O2k, Oxygraph-2k; OF, open field; OXPPOS, oxidative phosphorylation; P, OXPPOS; PFA, paraformaldehyde; PO<sub>2</sub>, partial pressure of oxygen; ROI, region of interest; ROX, residual oxygen consumption; S1FL, somatosensory (forelimb) region of the cortex; SO<sub>2</sub>, tissue oxygen saturation; SUIT, substrate, uncoupler, inhibitor titration.

## Financial support

This study was supported by the internal funding of UNIL allocated to LP and the allocated project funding for AH from The Roger Williams Institute of Hepatology, Foundation for Liver Research. CD was supported by the Swiss National Science Foundation under grant agreement no 194964.

## Conflicts of interest

RJ has research collaborations with Takeda and Yaqrit and consults for Yaqrit. RJ is the founder of Yaqrit Limited, which is developing UCL inventions for treatment of individuals with cirrhosis. RJ is an inventor of ornithine phenylacetate, which was licensed by UCL to Mallinckrodt. He is also the inventor of Yaq-001, DIALIVE, and Yaq-005, the patents for which have been licensed by his University into a UCL spinout company, Yaqrit Ltd. All other authors report no conflicts of interest. Please refer to the accompanying ICMJE disclosure forms for further details.

## Authors' contributions

Study concept and design: AH, LP. Acquisition of data: AH, CK, JK, ALG, PSH, SL. Analysis and interpretation of data: AH, JK, CD, IJC, KM, RCP. Drafting of the manuscript: AH. Critical revision of the manuscript for important intellectual content: AH, LP, RJ. Statistical analysis: AH. Obtained funding: AH, LP. Administrative, technical, or material support: CK, CD, MM, RJ, AK, US, RCP. Study supervision: AH, LP.

## Data availability statement

The data that support the findings of this study are available from the corresponding authors upon reasonable request.

## Acknowledgements

The authors are grateful to the colleagues from UNIL, Dr Nadège Zanou, Dr Sylviane Lagarigue, Cendrine Repond, Dr Marie-Laure Possovre, Dr Charlotte Jollé, and Cathy Gouelle, for their help with animal husbandry and knowledge exchange, as well as technical advice and stimulating discussions about the project. The authors would also like to acknowledge Mark Augath and Dr Ruiqing Ni for their technical support with MRI and multispectral optoacoustic tomography performed at ETH, as well as Dr Alexandre Sarre and Dr Corrine Berthonneche for their services of blood pressure measurements performed at UNIL. We are also very grateful to Prof. Alexander Gourine, who provided the equipment for the optical fluorescence oxygen measurements, as well as Dr Antonio Riva for his advice on cytokine selection. We thank the Wohl Cellular Imaging Centre at King's College London for help with confocal microscopy. Finally, we are thankful to Prof. Bengt Kayser and Prof. Nicolas Place (Institute of Sports Science and Department of Biomedical Sciences, University of Lausanne, Lausanne 1005, Switzerland) for their provision of the O2k machine and

reagents used in the Oroboros experiments, as well as Stijn den Daas and Dr Svetlana Mastitskaya for their efforts on the ImageJ plug in and antibody selection.

## Supplementary data

Supplementary data to this article can be found online at <https://doi.org/10.1016/j.jhep.2022.08.008>.

## References

Author names in bold designate shared co-first authorship

- [1] Byrne CD, Targher G. NAFLD: a multisystem disease. *J Hepatol* 2015;62(Suppl. 1):S47–S64.
- [2] Sanyal AJ, Van Natta ML, Clark J, Neuschwander-Tetri BA, Diehl A, Dasarthy S, et al. Prospective study of outcomes in adults with nonalcoholic fatty liver disease. *N Engl J Med* 2021;385:1559–1569.
- [3] Kanoski SE, Davidson TL. Different patterns of memory impairments accompany short- and longer-term maintenance on a high-energy diet. *J Exp Psychol Anim Behav Process* 2010;36:313–319.
- [4] Filipović B, Marković O, Đurić V, Filipović B. Cognitive changes and brain volume reduction in patients with nonalcoholic fatty liver disease. *Can J Gastroenterol Hepatol* 2018;2018:9638797.
- [5] Takahashi A, Kono S, Wada A, Oshima S, Abe K, Imaizumi H, et al. Reduced brain activity in female patients with non-alcoholic fatty liver disease as measured by near-infrared spectroscopy. *PLoS One* 2017;12:e0174169.
- [6] Colognesi M, Gabbia D, De Martin S. Depression and cognitive impairment-extrahepatic manifestations of NAFLD and NASH. *Biomedicines* 2020;8:229.
- [7] VanWagner LB, Terry JG, Chow LS, Alman AC, Kang H, Ingram KH, et al. Nonalcoholic fatty liver disease and measures of early brain health in middle-aged adults: the CARDIA study. *Obesity (Silver Spring)* 2017;25:642–651.
- [8] Kjærgaard K, Mikkelsen ACD, Wernberg CW, Grønkrjær LL, Eriksen PL, Damholdt MF, et al. Cognitive dysfunction in non-alcoholic fatty liver disease – current knowledge, mechanisms and perspectives. *J Clin Med* 2021;10:673.
- [9] Hosford PS, Gourine AV. What is the key mediator of the neurovascular coupling response? *Neurosci Biobehav Rev* 2019;96:174–181.
- [10] Raichle ME. The pathophysiology of brain ischemia. *Ann Neurol* 1983;13:2–10.
- [11] Halder SK, Milner R. Hypoxia in multiple sclerosis; is it the chicken or the egg? *Brain* 2021;144:402–410.
- [12] Jiyeon O, Cho H-J, Hong SH, Kim IK, Suk K. Hypoxia as an initiator of neuroinflammation: microglial connections. *Curr Neuropharmacol* 2005;3:183–191.
- [13] DiSabato DJ, Quan N, Godbout JP. Neuroinflammation: the devil is in the details. *J Neurochem* 2016;139(Suppl. 2):136–153.
- [14] Moreno-Navarrete JM, Blasco G, Puig J, Biamés C, Rivero M, Gich J, et al. Neuroinflammation in obesity: circulating lipopolysaccharide-binding protein associates with brain structure and cognitive performance. *Int J Obes (Lond)* 2017;41:1627–1635.
- [15] Pierre K, Pellerin L. Monocarboxylate transporters in the central nervous system: distribution, regulation and function. *J Neurochem* 2005;94:1–14.
- [16] Carneiro L, Asrih M, Repond C, Sempoux C, Stehle JC, Leloup C, et al. AMPK activation caused by reduced liver lactate metabolism protects against hepatic steatosis in MCT1 haploinsufficient mice. *Mol Metab* 2017;6:1625–1633.
- [17] **Lengacher S, Nehiri-Sitayeb T**, Steiner N, Carneiro L, Favrod C, Preitner F, et al. Resistance to diet-induced obesity and associated metabolic perturbations in haploinsufficient monocarboxylate transporter 1 mice. *PLoS One* 2013;8:e82505.
- [18] Percie du Sert N, Hurst V, Ahluwalia A, Alam S, Avey MT, Baker M, et al. The ARRIVE guidelines 2.0: updated guidelines for reporting animal research. *PLoS Biol* 2020;18:e3000410.
- [19] Sitar-Taut AV, Cozma A, Fodor A, Coste SC, Orasan OH, Negrean V, et al. New insights on the relationship between leptin, ghrelin, and leptin/ghrelin

- ratio enforced by body mass index in obesity and diabetes. *Bio-medicines* 2021;9:1657.
- [20] Leyh J, Winter K, Reinicke M, Ceglarek U, Bechmann I, Landmann J. Long-term diet-induced obesity does not lead to learning and memory impairment in adult mice. *PLoS One* 2021;16:e0257921.
- [21] Xia G, Han Y, Meng F, He Y, Srisai D, Farias M, et al. Reciprocal control of obesity and anxiety-depressive disorder via a GABA and serotonin neural circuit. *Mol Psychiatry* 2021;26:2837–2853.
- [22] Xiao J, Lim LKE, Ng CH, Tan DJH, Lim WH, Ho CSH, et al. Is fatty liver associated with depression? A meta-analysis and systematic review on the prevalence, risk factors, and outcomes of depression and non-alcoholic fatty liver disease. *Front Med (Lausanne)* 2021;8:691696.
- [23] Luci C, Bourinet M, Leclère PS, Anty R, Gual P. Chronic inflammation in non-alcoholic steatohepatitis: molecular mechanisms and therapeutic strategies. *Front Endocrinol (Lausanne)* 2020;11:597648.
- [24] Dorfman MD, Thaler JP. Hypothalamic inflammation and gliosis in obesity. *Curr Opin Endocrinol Diabetes Obes* 2015;22:325–330.
- [25] Balzano T, Forteza J, Molina P, Giner J, Monzó A, Sancho-Jiménez J, et al. The cerebellum of patients with steatohepatitis shows lymphocyte infiltration, microglial activation and loss of purkinje and granular neurons. *Sci Rep* 2018;8:3004.
- [26] Norden DM, Fenn AM, Dugan A, Godbout JP. TGF $\beta$  produced by IL-10 redirected astrocytes attenuates microglial activation. *Glia* 2014;62:881–895.
- [27] Ding X, Yan Y, Li X, Li K, Ciric B, Yang J, et al. Silencing IFN- $\gamma$  binding/signaling in astrocytes versus microglia leads to opposite effects on central nervous system autoimmunity. *J Immunol* 2015;194:4251–4264.
- [28] Guillemot-Legris O, Muccioli GG. Obesity-induced neuroinflammation: beyond the hypothalamus. *Trends Neurosci* 2017;40:237–253.
- [29] Pellerin L, Pellegrini G, Martin JL, Magistretti PJ. Expression of monocarboxylate transporter mRNAs in mouse brain: support for a distinct role of lactate as an energy substrate for the neonatal vs. adult brain. *Proc Natl Acad Sci U S A* 1998;95:3990–3995.
- [30] Kong L, Wang Z, Liang X, Wang Y, Gao L, Ma C. Monocarboxylate transporter 1 promotes classical microglial activation and pro-inflammatory effect via 6-phosphofructo-2-kinase/fructose-2, 6-biphosphatase 3. *J Neuroinflammation* 2019;16:240.
- [31] Moreira TJ, Pierre K, Maekawa F, Repond C, Cebere A, Liljequist S, et al. Enhanced cerebral expression of MCT1 and MCT2 in a rat ischemia model occurs in activated microglial cells. *J Cereb Blood Flow Metab* 2009;29:1273–1283.
- [32] Perry VH. The influence of systemic inflammation on inflammation in the brain: implications for chronic neurodegenerative disease. *Brain Behav Immun* 2004;18:407–413.
- [33] Mukandala G, Tynan R, Lanigan S, O'Connor JJ. The effects of hypoxia and inflammation on synaptic signaling in the CNS. *Brain Sci* 2016;6:6.
- [34] Lombardi R, Fargion S, Fracanzani AL. Brain involvement in non-alcoholic fatty liver disease (NAFLD): a systematic review. *Dig Liver Dis* 2019;51:1214–1222.
- [35] Institoris A, Gordon GR. A tense relationship between capillaries and pericytes. *Nat Neurosci* 2021;24:615–617.
- [36] Laferriere CA, Pang DS. Review of intraperitoneal injection of sodium pentobarbital as a method of euthanasia in laboratory rodents. *J Am Assoc Lab Anim Sci* 2020;59:254–263.
- [37] Halestrap AP, Price NT. The proton-linked monocarboxylate transporter (MCT) family: structure, function and regulation. *Biochem J* 1999;343:281–299.
- [38] Weiss HJ, Angiari S. Metabolite transporters as regulators of immunity. *Metabolites* 2020;10:418.
- [39] **Perez-Escuredo J, Van Hée VF, Sboarina M, Falces J, Payen VL, Pellerin L, et al.** Monocarboxylate transporters in the brain and in cancer. *Biochim Biophys Acta* 2016;1863:2481–2497.
- [40] Elizondo-Vega R, Cortes-Campos C, Barahona MJ, Oyarce KA, Carril CA, García-Robles MA. The role of tanycytes in hypothalamic glucosensing. *J Cell Mol Med* 2015;19:1471–1482.
- [41] Geller S, Arribat Y, Netzahualcoyotzi C, Lagarrigue S, Carneiro L, Zhang L, et al. Tanycytes regulate lipid homeostasis by sensing free fatty acids and signaling to key hypothalamic neuronal populations via FGF21 secretion. *Cell Metab* 2019;30:833–844.e7.
- [42] Hadjihambi A. Cerebrovascular alterations in NAFLD: is it increasing our risk of Alzheimer's disease? *Anal Biochem* 2021;636:114387.